Occurrence and Spatial Distribution of the Neutral Per-fluoroalkyl Substances, and Cyclic Volatile Methylsiloxanes in Atmosphere of the Tibetan Plateau

Xiaoping Wang[1,2], Jasmin Schuster[3,4], Kevin C. Jones[4], and Ping Gong[1,2]*

[1]Key Laboratory of Tibetan Environment Changes and Land Surface Processes, Institute of Tibetan Plateau Research, Chinese Academy of Sciences, Beijing, 100101, China

[2]CAS Center for Excellence in Tibetan Plateau Earth Sciences，Beijing, 100101, China

[3]Air Quality Processes Research Section, Environment and Climate Change Canada, 4905 Dufferin St., Toronto, ON M3H 5T4, Canada

[4]Lancaster Environment Centre, Lancaster University, Lancaster, LA1 4YQ, U.K.

*** Corresponding author address:**

E-mail: wangxp@itpcas.ac.cn

Tel: +86-10-84097120

Fax: +86-10-84097079

Abstract

Due to their properties of bioaccumulation, toxicity, and long-range atmospheric transport, poly and per-fluoroalkylsubstances (PFASs), and cyclic volatile methyl siloxanes (cVMS) are currently being considered as emerging persistent organic pollutants (POPs) for regulation. To date, there are limited data on PFASs and cVMS in the atmosphere of the Tibetan Plateau (TP), a remote environment which can provide information on global background conditions. Sorbent-impregnated polyurethane foam (SIP) disk passive air samplers were therefore deployed for three months (May to July 2011 and 2013) at 16 locations across the TP. Using previously reported methods for estimating the air volume sampled by SIP disks, the derived atmospheric concentrations ranged as follows: 18–565 ng/m^3 for ΣcVMS (including D3, D4, D5, and D6); 65–223 pg/m^3 for fluorotelomer alcohols (ΣFTOHs); 1.2–12.8 pg/m^3 for fluorinated sulfonamides (ΣFOSA); and 0.29–1.02 pg/m^3 for fluorinated sulfonamidoethanols (ΣFOSE). The highest ΣcVMS occurred at Lhasa, the capital city of the TP, indicating the local contribution to the emerging pollutants. Higher levels of ΣFTOHs were observed at sites close to the transport channel of the Yarlung Tsangpo Grand Canyon, indicating possible long-range atmospheric transport (LRAT). Elevated concentrations of shorter-chain volatile PFAS precursors (4:2 FTOH and fluorobutane sulfonamidoethanol) were found in most air samples, reflecting the shift in production from long- to short-chain PFASs in Asia. Overall, concentrations of emerging POPs at background sites of the TP were 1–3 orders of magnitude higher than those reported for legacy POPs.

Introduction

Persistent organic pollutants (POPs) have attracted significant attention due to their wide distribution in the environment and high toxicity to humans and wildlife (Hung et al., 2016a; Hung et al., 2016b; Magulova and Priceputu, 2016; Rigét et al., 2010). In the first stage, the Stockholm Convention included twelve POPs, normally considered the legacy POPs (Rigét et al., 2010), including dichlorodiphenyltrichloroethane (DDT), hexachlorobenzene (HCB), and hexachlorocyclohexanes (HCHs). With the prohibition of these legacy POPs, their levels in the environment have largely deceased (Hung et al., 2016a; Hung et al., 2016b). Compared with these legacy POPs, other organic substances, such as per-fluoroalkyl substances (PFASs), and volatile methyl-siloxanes (VMS), have attracted more attention in recent years in the environmental chemistry research community (Pedersen et al., 2016; Shi et al., 2015; Wang et al., 2015a; Xiao et al., 2015) due to their widespread production, bioaccumulative behavior, and toxicity. In 2009, perfluorooctanesulfonic acid (PFOS) and perfluorooctane sulfonyl fluoride (POSF)-based chemicals were listed under Annex B of the restricted substances of the Stockholm Convention (Zushi et al., 2012).

In addition, use of VMS in personal care products have also been restricted by the European Chemical Agency (ECHA, 2012). Due to their widespread use in inks, waxes, firefighting foams, metal plating and cleaning, coating formulations, and repellents for leather, paper, and textiles, large quantities of PFASs have been discharged into the environment (Shoeib et al., 2006). Taking PFOS as an example, the total historical worldwide production of "PFOS equivalent", including secondary reaction products and precursors, was estimated to be 122,500 tons between 1970 and 2002 (Guerranti et al., 2013; Paul et al., 2009). However, since 2002, the emission of PFASs has shifted from North America, Europe, and Japan to emerging Asian economies, especially China and India (Li et al., 2011; Sharma et al., 2016). Passive air sampling results have found that fluorotelomer alcohols (FTOH) and fluorinated telomere olefins (FTO) are major compound classes occurring in the urban air of China and Japan, while 4:2 FTOH

is a predominant chemical in remote regions of China and India (Li et al., 2011).

Methylsiloxanes are widely used in industrial and commercial applications, including additives in fuel, car polish, cleaners, waxes, and personal care products (cosmetics, deodorants and lotions, Borga et al., 2013; Buser et al., 2013). Cyclic volatile methylsiloxanes (cVMS) include hexamethylcyclotrisiloxane (D3), octamethylcyclotetrasiloxane (D4), and their rearrangement products such as decamethylcyclopentasiloxane (D5) and dodecamethylcyclohexasiloxane (D6). These chemicals are the subject of increasing concern because of their high emissions, long persistence (Navea et al., 2011), and toxicities (Mackay et al., 2015). D4 and D5 have been categorized as high production volume chemicals (McLachlan et al., 2010) and identified as new persistent and bioaccumulative chemicals in commerce (Borga et al., 2013; McGoldrick et al., 2014). Due to the high volatility, VMS can be released into the atmosphere during use and production (Xu et al., 2014). The half-lives of VMS in the atmosphere range from days to weeks (Xu et al., 2014; Xu and Wania, 2013), which allow them to undergo long-range atmospheric transport (LRAT) and arrive at remote regions such as the Arctic and Antarctic.

Despite of the minor local emissions, remote regions can also receive pollutants by LRAT and the contamination levels of pollutants in these areas reflect the extent to which the remote area has been contaminated. Studies on the occurrence and distribution of PFASs and cVMS have been conducted in various environmental media of the Arctic (Krogseth et al., 2013) and Antarctic (Sanchís et al., 2015), where unexpectedly high concentrations were found. As well as the Arctic and Antarctic, the Tibetan Plateau (TP) is often referred to as the “third pole”, isolated in the mid-latitude northern hemisphere with a harsh environment and high elevation. The transport (Sheng et al., 2013), distribution (Wang et al., 2010; 2016b), and bioaccumulation (Ren et al., 2016) of legacy POPs in the Tibetan environment have already been investigated; however, there is still a gap in knowledge regarding the distribution of emerging organic contaminants, such as PFASs and cVMS.

In this study, sorbent-impregnated polyurethane foam (SIP) disk passive air samplers were deployed across the TP (16 sites) to obtain the spatial distribution of PFASs and cVMS in the atmosphere. These sites include densely populated cities and background sites, in order to test how the local emission and LRAT contaminate the TP. Combining the results of this study with the published data regarding legacy POPs in the TP, and emerging POPs in other Asian regions, will provide useful insights to understand the exposure risks of legacy and emerging POPs in the Tibetan environment, and gain a comprehensive understanding of the distribution pattern of emerging POPs in Asia.

Materials and methods

Preparation of SIPs. Air monitoring in remote areas is especially challenging due to the lack of electricity. Passive air samplers (PAS) have the advantage that they do not require electricity, and are also cheap and easy to handle. Among the various PAS, SIP uses polyurethane foam (PUF) coated with polystyrene divinylbenzene copolymeric resin (XAD-4) as the absorption medium, which has been widely used for a range of POPs, including PFASs, VMS, and PCBs (Ahrens et al., 2013; Genualdi et al., 2010, 2011; Shoeib et al., 2008). The preparation of SIP was conducted at Lancaster University, U.K., following the previously published method (Shoeib et al., 2008). Briefly, PUF disks (Tisch Environmental) were pre-extracted in a Soxhlet with acetone (12 h) and petroleum ether (18 h). Amberlite XAD-4 was precleaned by sonication in methanol, dichloromethane, and hexane (30 min each). The precleaned Amberlite XAD-4 was ground to a powder using a Retsch planetary ball mill (particle diameter approximately 0.75 μm). The PUF disks were coated with the XAD-4 by dipping the precleaned disks in a dispersion of the powdered Amberlite XAD-4 slurry in hexane. SIP-PUF disks were dried under vacuum, and an average of 435 ± 30 mg of XAD-4 coated each disk (n = 80; each sampling had 32 samples and 8 field blanks), which was similar to the Global Passive Atmospheric Sampling program (Genualdi et al., 2010). All prepared SIP disks were stored in sealed metal tins at −17°C until they were transferred to the sampling locations.

Sampling campaign

Taking advantage of the Tibetan Observation and Research Platform (Wang et al., 2016a), a passive air monitoring network comprising 16 sampling sites across the TP has been established, with good spatial coverage of the TP (Supporting Information, Fig. S1), and has already produced results regarding the spatial and temporal pattern of legacy POPs (Wang et al., 2010; 2016b). In this study, duplicate SIP-PAS were deployed at each sampling site for about 100 days from May to July for sampling PFASs (2011) and cVMS (2013). During the sampling, another PUF sampler was co-deployed to obtain the site-specific sampling rate using four depuration compounds (DCs; PCB-30, -54,-104, and -188; Pozo et al., 2009). Details relating to the DCs can be found in Text S1. The sampling program and meteorological conditions at each site are provided in Table 1. Field blanks were unpacked and exposed them in air for 1 min at the sampling site and then treated as real samples. At the end of the deployment period, the collected SIP-PUF and PUF disks were sealed in metal tins and transported to the clean lab in Lhasa for extraction.

Sample extraction and analysis

The target PFASs were neutral PFASs, including fluorotelomer olefin (8:2 FTO), fluorotelomer acrylates (6:2, 8:2 FTA), fluorotelomer alcohols (4:2, 6:2, 8:2, 10:2, and 12:2 FTOH), sulfonamides (NMeFBSA, NMeFOSA, and NEtFOSA), and sulfonamidoethanols (NMeFBSE, NMeFOSE, and NEtFOSE); the four target cVMS were D3, D4, D5, and D6. PFAS standards were purchased from Wellington Laboratories Inc. (Guelph, Ontario, Canada), and D3, D4, D5, and D6 were purchased from Tokyo Chemical Industries America (Portland, OR).

Extraction of the PFASs was performed by sequential cold column extraction with ethyl acetate as the extraction solvent. Field blanks and lab blanks were extracted along with samples in the same way. After the spiking of the recovery standard (see Table S1 for the composition), SIP was extracted by three separate immersions (30 min) in ethyl

156 acetate, and all three extracts were combined and concentrated. These extracts were
157 then filtered by Millipore Millex syringe filter unite (0.45µm, 4mm), reduced to a
158 volume of 1 ml and cleaned up by 2 cm of Envi-Carb. Finally, after adding the internal
159 standard (Table S1), the extracts were reduced to 50 µl for injection. The analysis of
160 volatile PFASs was performed using GC-MS equipped with a SUPELCO WAX
161 column (60 m, 0.25 mm inner diameter, 0.25 µm film, Supelco, Bellefonte, PA) under
162 positive chemical ionization mode. Details about the GC program is provided in Text
163 S2.
164 Before sampling, the SIP disks were spiked with recovery mixture containing each of
165 the ^{13}C4-D4, ^{13}C5-D5, and ^{13}C6-D6, and after sampling, they were Soxhlet extracted
166 with petroleum ether/acetone (85/15, v/v) for around 6 h. All extracts were then
167 concentrated by rotary evaporation, followed by gentle nitrogen blow-down to 0.5 mL
168 using isooctane as a keeper for the extracts. Mirex was added to the final extract as an
169 internal standard. The separation and detection of the cVMSs was performed using GC-
170 MS in selective ion monitoring mode using a DB-5 column (60 m, 0.25 mm inner
171 diameter, 0.25 µm film, J&W Scientific). Methods regarding GC program and MS
172 detection ions are provided in Text S2.

173

174 **Quality assurance/quality control**

175 Samples were extracted in a clean lab with filtered, charcoal stripped air and positive
176 pressure conditions. All glassware used for sample collection was cleaned, and baked
177 at 450°C before use. Powder-free nitrile gloves were used for all handling of the
178 samples. All personnel involved in sample collection and analysis refrained from using
179 personal care products to avoid contamination. A total of eight field blanks and six lab
180 blanks were analyzed for target PFASs. In the lab blanks, only 8:2 FTOH and 10:2
181 FTOH were screened, which showed low concentrations, while 4:2 FTOH, 8:2 FTOH,
182 10:2FTOH, NEtFOSA, NMeFOSE, and NEtFOSE were observed in field blanks, with
183 concentrations ranging between 50 and 321 pg/sample (Table S2). Similarly, eight field

184 blanks and six lab blanks were arranged for evaluating the uncertainties of cVMS
185 concentrations due to contamination and loss processes (during the extraction and
186 cleanup procedures and storage). D3, D4, D5, and D6 in field blanks were, on average,
187 34, 57, 380, and 59 ng/sample, respectively, which were approximately 6% of the
188 sample concentration. Method detection limits (MDLs) were calculated from the blanks
189 [average of blanks + 3 × standard deviation (σ)]. Based on this principle, MDLs of
190 volatile PFASs ranged between 37 and 419 pg/sample, while MDLs of cVMS ranged
191 between 52 and 681 ng/sample (Table S3). Details of the MDLs for each congener are
192 provided in Table S2 and S3.

193 The average recoveries of internal standard were 88 ± 27%, 79 ± 34%, 71 ± 27%, 95 ±
194 21%, and 107 ± 19% for 5:1 FTOH, 7:1FTOH, [M+5]8:2 FTOH, 9:1 FTOH, and 11:1
195 FTOH, respectively; and 117 ± 33%, 105 ± 27%, 89 ± 37%, 93 ± 33%, and 92 ± 29%
196 for [M+3]NMeFOSA, [M+5]NEtFOSA, [M+7]NMeFOSE, and [M+9]NEtFOSE,
197 respectively. These recoveries were broadly in line with previous passive air sampling
198 for Asian counties in which the same SIP disks were deployed (Li et al., 2011). The
199 recoveries were 116.0 ± 5.9%, 90 ± 8.5%, and 98.2 ± 1.7% for ^{13}C-D4, ^{13}C-D5, and
200 ^{13}C-D6, respectively.

201 **Sampling rate calculation**

202 Generally, the uptake profile of a chemical to the passive sampler medium (PSM)
203 includes three stages: 1) quick, linear uptake when the amount of chemicals in the PSM
204 is small; 2) curvilinear uptake (slow uptake); and 3) equilibrium uptake when the
205 amount of chemicals in the PSM reaches a plateau. Volatile compounds usually have
206 short linear phase absorption and equilibrate after a few weeks in SIP (Ahrens et al.,
207 2013; Shoeib et al., 2008), while longer linear phases will occur if SIP is operated at
208 colder temperatures (Ahrens et al., 2013). In a previous calibration study (in which the
209 sampling temperature was 18°C), linear phase uptake of PFASs in SIP was reported
210 (Ahrens et al., 2013), due to the greater capacity of SIP-PAS to PFASs. However, the
211 sampling temperature in the present study (Table 1) was much lower, and so linear

phase absorption should be expected to occur. For this reason, the previously reported average linear sampling rate (R) of 4 m^3d^{-1} reported by Ahrens et al (2013) for PFASs (including FTOHs, FOSAs and FOSE) was chosen to estimate the final sample air volume of the SIP-PAS (multiplying 4 m^3d^{-1} by the number of days of deployment). Based on this estimation, volumetric concentrations of target compounds were obtained and are presented in Table S4. The MDLs in Table S4 were also calculated based on the 90-day exposure duration.

The volume of air sampled for cVMS in SIP disks can be described by the following equation:

$$V_{air} = K_{SIP-A} \times V_{SIP} \times (1 - \exp\{-(A_{SIP})/(V_{SIP}) \times (k_A/K_{SIP-A})\}t) \qquad (1)$$

where V_{air} is the air volume sampled by the SIP disk, $K_{SIP\text{-}A}$ is the SIP-air partition coefficient, V_{SIP} is the volume of the SIP disk (cm^3), A_{SIP} is the planar surface area of the SIP disk (cm^2), k_A is the air-side mass transfer coefficient (m/day), and t is deployment time (days). $K_{SIP\text{-}A}$ is highly temperature dependent and can be calculated using its correlations with K_{OA} (Ahrens et al., 2014). Details about the calculation are presented in Table S5. Values of k_A can be derived from the site-specific sampling rate (Rs) and the surface area of the SIP disk (A_{SIP}). The Rs values were calculated from the use of DCs on the PUF disks that were co-deployed at each site. Details of these calculations have been previously reported and are presented in Text S2 and Table S6. The values of log ($K_{SIP\text{-}A}$) for D3, D4, D5, and D6 are listed in Table S7; and the air volume sampled by the SIP disk are provided in Table S8. Then, volumetric concentrations of D4, D5, and D6 are presented in Table S9.

Result and discussion

Concentration of neutral PFASs and cVMS

From Table S5, with the exception of fluorotelomer acrylates (6:2, 8:2 FTA), all neutral PFAS congeners were quantitatively detected in all samples. This implies that the

neutral PFAS were ubiquitous in the air of the TP. The dominant compounds were FT alcohols, with the total concentration of FTOH (sum of 4:2 FTOH, 6:2 FTOH, 8:2 FTOH, 10:2 FTOH and 12:2 FTOH) ranging from 65 to 223 pg/m^3. These values are lower than those measured in Chinese cities, such as Beijing, Taiyuan, and Changsa (Li et al., 2011) but are higher than those reported at background sites, including remote mountains in China (80–120 pg/m^3, Li et al., 2011), Antarctica (13.5–46.9 pg/m^3, Wang et al., 2015b), and the Arctic (7.7–49 pg/m^3, Shoeib et al., 2006). Among all the FTOHs, concentrations of 8:2 and 4:2 FTOH were the highest, being in the tens of (up to one hundred) pg/m^3. Generally, 8:2 FTOH was the prevailing compound found in the gas phase. This may be due to its relatively high volatility and long atmospheric lifetime (Rayne et al., 2009). However, concentrations of 8:2 FTO were in the range of 0.88 to 4.56 pg/m^3, which are lower than those measured in other background regions (~ tens of pg/m^3, Li et al., 2011). Levels of fluorinated sulfonamides (sum of NMeFBSA, NMeFOSA, and NEtFOSA) in Table S4 can reach a maximum of around 10 pg/m^3, while the total concentration of sulfonamidoethanols (including NMeFBSE, NMeFOSE, and NEtFOSE) was only a few pg/m^3, which is an order of magnitude lower than those observed for sulfonamides. It is clear that the proportion of FTOHs was much higher than FOSEs and FOSAs, which may be due to FOSEs and FOSAs being prone to absorption on particles (Li et al., 2011). This can also be caused by different phasing-out time for these chemicals. Products containing FOSEs and FOSAs were mostly produced by 3M and mostly phased out in 2002, while, products releasing 8:2 FTOH were more recently phased out.

The measurements reported here represent the first survey of concentrations of cVMS in the TP (also known as “the Third Pole”, Qiu, 2008). All measured cVMS concentrations were above the MDL, suggesting cVMS were also ubiquitous in the Tibetan atmosphere (Table S6). The average atmospheric concentrations for D3, D4, D5, and D6 were 29.1, 38.8, 88.6 and 1.6 ng/m^3, respectively (Table S9). Concentrations of D5 were higher than D3 and D4, which is different from the reported concentrations of 17, 16, 4.0, and 0.54 ng/m^3 for D3, D4, D5, and D6 at the Zeppelin

observatory (Arctic) using the same SIP-disks for sampling (Genualdi et al., 2011). However, similar to other Arctic results, D5 was the dominant congener in air (Krogseth et al., 2013). D5 is the most frequently used cVMS in personal care products, and therefore is the predominant cVMS in the urban atmosphere (McLachlan et al., 2010). However, dominance of D5 have been observed in both Arctic and Antarctic region, highlighting its persistence in atmosphere and LRAT potential. The obtained cVMS concentrations in the TP are higher than those reported for Arctic and remote Sweden, indicating the possible local contamination. Both PFASs and cVMS are closely associated with human activities, and their concentrations usually show positive correlations with population (Genualdi et al., 2010; Nguyen et al., 2016). Therefore, we would expect high concentrations of volatile PFASs and cVMs in the atmosphere of Lhasa and Golmud, which are the two largest cities on the TP, with relatively large populations and fast urbanization. From Table S4 and S9, in Lhasa (the capital and also the largest city of the Tibet autonomous region), the concentrations of 8:2 FTOH and 4:2 FTOH were 71 and 43 pg/m^3, respectively, and similar levels were also found for Golmud. Additionally, concentrations of D5 in Lhasa and Golmud were 465 and 208 ng/m^3 respectively, which were the two highest D5 concentrations in the Tibetan atmosphere (Table S10). Although these levels were still orders of magnitude lower than those reported for other megacities (Genualdi et al., 2010; Mackay, 2015) the elevated concentrations suggest that the expansion/development of cities, followed by the migration of rural populations, may lead to an increase of emerging pollutants in Tibet.

Spatial distribution and congener profile of neutral PFASs

An important objective of this study was to improve knowledge on the spatial patterns of emerging POPs in the background air across the TP. In previous studies, the spatial distributions of atmospheric legacy organochlorine pesticides over the TP have been reported, and were found to be strongly related to the air circulation patterns of the TP, i.e. the Indian Monsoon and westerly winds (Figure S2, Wang et al., 2010; 2016b). For example, DDT-related chemicals were major chemicals in the atmosphere of the

296 southeastern TP, which is influenced by the Indian monsoon air masses (Wang et al.,
297 2010); whereas, the northwestern TP was dominated by HCB in the atmosphere, caused
298 by the westerly-driven European air masses (Wang et al., 2016b). Similarly, ice cores
299 collected in different regions of the TP indicated that PFOS existed in the Muztagata
300 glacier (western TP); while in the Zuoqiupu glacier, located in the eastern TP, PFOS
301 was below the detection limit, but concentrations of short-chain perfluorobutanoic acid
302 have increased during recent years (Wang et al., 2014). All these results suggest that
303 differences in the concentrations and composition profiles of POPs likely reflect the
304 upwind sources affecting the different parts of the TP (e.g., European/central Asian
305 sources for the west TP and Indian sources for the east TP).

306 Figure 1 presents the spatial patterns of 8:2 FTO, FTOHs, FOSAs, and FOSEs. The
307 spatial distribution of 8:2 FTO shows a decreasing gradient from the east to the west of
308 the TP (Figure 1). One-way analysis of variance (ANOVA) was performed to determine
309 the statistical differences in the values of individual chemicals among different
310 sampling sites. If the *p*- value is lower than 0.05, we conclude the significant differences
311 occur. On the basis of the ANOVA results, significantly high values of 8:2 FTO were
312 found at Qamdo and Bomi (Table S10). However, spatial variation was found in total
313 FTOHs (Figure 1), and significant differences only occurred at the east regions (Chayu,
314 Rawu, and Lulang) and the western sites (Gar and Muztagata, Table S7). It is noted that
315 the highest ΣFTOH concentration occurred at Chayu (222 pg/m^3), which is on the
316 southern slopes of the Himalaya and close to the China–India border. Levels of
317 ΣFTOHs in Chayu were even higher than that of Lhasa (180 pg/m^3), suggesting that the
318 southeast part of the TP may receive considerable inputs of PFASs from south Asia.
319 Regarding ΣFOSAs and ΣFOSEs, higher levels were seen in both the east and west of
320 the TP (Figure 1), compared to the middle of the TP. A previous study observed high
321 levels of atmospheric DDTs at sites (e.g. Chayu, Rawu, Bomi, etc.) close to the Yarlung
322 Tsangpo Grand Canyon (Wang et al., 2016b). Here, ΣFTOHs, ΣFOSAs, and ΣFOSEs
323 also showed higher levels at these sites (Figure 1), which confirms previous results that
324 show that the Yarlung Tsangpo Grand Canyon is a channel for receiving pollutants

from southern Asia (Sheng et al., 2013; Wang et al., 2016b). Medium ΣFOSA and ΣFOSE concentrations found in the Muztagata region broadly agree with the previous results that air masses originating from European sources are generally clean (Wang et al., 2016b).

As mentioned above, the composition profile of POPs is closely associated with air circulation patterns in the TP and can reflect the upwind sources. However, congener profiles of neutral PFASs in this study did not show any clear difference between western sites (e.g. Muztagata, Gar) and eastern sites (Chayu, Bomi, Lulang, etc.) (Figure 1), which may be because the sampling period was too short (~ 3 months) and only covered the monsoon season (June to September). Elevated 4:2 FTOH and NMeFBSE concentrations were found in most of the samples of the present study and a dominance of shorter-chain volatile PFAS precursors was the feature of the south Asian sources (Li et al., 2011). This similarity suggests that neutral PFASs in the TP may originate mainly from south Asia, most likely by LRAT.

Although the congener profiles cannot be used to distinguish the European and Indian sources in this study, the ratio of 8:2 to 10:2 to 6:2 FTOH is an excellent indicator of LRAT for atmospheric PFASs (Wang et al., 2015b). The transport fate of atmospheric PFASs can be influenced by photochemical degradation. A higher ratio indicates the aged nature of the air mass because of the fast photochemical degradation of 6:2 FTOH (half-life = 50 days) in the air compared with 10:2 FTOH (70 days) and 8:2 FTOH (80 days, Piekarz et al., 2007). During LRAT, more 6:2 and 10:2 FTOH will be removed from the atmosphere. For example, ratios of 6.4:2.1:1.0 were observed in the Arctic (Ahrens et al., 2011) and 35.6:6.5:1.0 were found in the Antarctic (Wang et al., 2015b). In the present study, low ratios were observed in the cities, i.e. 2.4:1.7:1 and 6.8:1.2:1 were observed for Lhasa and Golmud, respectively. This indicates that cities are possible fresh emission sources of neutral PFASs. According to a previous study, there are three climate zones over the TP—namely, the monsoon region, westerly region, and transition region (Wang et al., 2016b). The sampling sites of this study can be grouped into these three zones (Figure S2, Table S11). The average ratios of 8:2 to 10:2 to 6:2

FTOH were 8.4:1.2:1 for the monsoon region, 8.8:1:1 for the westerly region and 10.6:1.2:1 for the transition zone (Figure S2, Table S11). Overall, these values are comparable to those reported for the Arctic. On the other hand, a decrease in 6:2 FTOH and an increase in 8:2 and 10:2 FTOH occurred from the edge regions to the central part of the TP (Table S11). The high ratios indicate the aged nature of atmospheric PFASs in the atmosphere of the TP, especially around the transition zone (Table S11). Given that the transition zone is located in the hinterland (central part) of Tibet, where both monsoon and westerly winds become week, and the fresh impact of source regions of either India or Europe/central Asia is limited, thus, the aged/old PFASs in the air of central TP is expected and reasonable.

Correlations between PFAS compounds

Correlations between concentrations of pollutants can be used to test if they have some common sources or undergo similar environmental fates. A correlation matrix was therefore prepared and showed that some chemicals were significantly correlated (Table 2). Good correlations ($r > 0.80$, $p < 0.01$) were observed between 8:2 FTOH and 10:2 FTOH ($r = 0.90$), and between 10:2 FTOH and 12:2 FTOH ($r = 0.97$). This phenomenon has been observed in other studies (Ahrens et al., 2012; Cai et al., 2012; Li et al., 2011) and usually suggests that 8:2 FTOH, 10:2 FTOH, and 12:2 FTOH have the same source. Correlations between 4:2 FTOH/6:2 FTOH and other FTOHs are generally low, or not significant, indicating 4:2 FTOH and 6:2 FTOH may come from different sources. There is much evidence that the manufacture of PFASs has shifted from longer-chain chemicals (C8 or above) to shorter-chain ones (C4 or C6, Butt et al., 2010; Hogue, 2012), which may lead to the poor correlation between short-chain FTOH and other FTOHs. Given the new production of shorter-chain PFASs mainly centered in Asian countries, such as China and India (Hogue, 2012) it is not surprising that high levels of both 4:2 FTOH and its independent characteristics have been found in the Tibetan atmosphere, due to the close proximity between Tibet and south Asia.

With regard to the relationships between FOSAs and FOSEs, good correlations were

seen among NMeFBSA, NMeFOSA, and NEtFOSA (Table 2). Additionally, concentrations of NMeFBSE were significantly correlated with those of NMeFOSE (Table 2). This is in contrast to previous results, in which poor relationships (r=0.283) were found between short- and long-chain PFASs (Li et al., 2011). Regarding the emission patterns of FOSAs and FOSEs in India, mixed manufacturing with both extensive emissions of NMeFOSA and NMeFOSE, coupled with wide discharge of NMeFBSA, have been reported in the Indian environment (Li et al., 2011). This indicates that both long- and short-chain PFAS are produced in south Asia. Favored by the transport of the Indian monsoon, the co-transport of short- and long-chain PFASs may lead to a blending of these chemicals in the Tibetan air. Meanwhile, the two short-chain PFASs, 4:2 FTOH and NMeFBSA, were significantly (r = 0.84, p < 0.01; Table 2) correlated with each other, suggesting these precursors may be released together in the source region.

Spatial distribution of cVMS across the TP

As mentioned above, greater levels of cVMS were found in the urban areas of Lhasa and Golmud. This can also be seen in the spatial map of cVMS (Figure 2). However, high levels of cVMS also occurred in the remote southeast of Tibet (Figure 2). Unlike the spatial pattern of neutral PFASs, concentrations of cVMS decreased from southeast to northwest TP (Figure 2, Table S9). Although there are no studies that report the cVMS levels and patterns in south Asian countries, due to the source of cVMS to the environment taking place via the use of personal care products we can expect the regions of south Asia (e.g. the Indo-Gangetic Plain), with its high population density, to be important cVMS source regions. The close proximity of the southeast TP to south Asia and the fast LRAT potential of cVMS (Xu et al., 2014; Xu and Wania, 2013) might be the reason that high concentrations of cVMS occur in the southeast TP. On the other hand, latitude might be a factor representing the influence of the emission source on the spatial pattern.

Another reason that can also influence the atmospheric concentration of cVMS is their

atmospheric degradation by hydroxyl radicals. In the Arctic, low levels of hydroxyl radicals during the polar night promotes the accumulation of cVMS in the air, while the polar day enhances the degradation, causing the strong seasonality of cVMS in the Arctic (Krogseth et al., 2013). The polar day usually increases hydroxyl radicals in the air and enhances the photo-degradation of contaminants (Krogseth et al., 2013). The level of hydroxyl radicals is generally proportional to the extent of solar UV radiation (Rohrer and Berresheim, 2006). Recently, Liu et al. (2017) published two UV radiation datasets that cover the whole of China, and high values were observed for the south TP, with a gradual decrease from the south to the north TP. Although the sampling sites in their study were not exactly the same as in our study, their spatial trend of UV radiation suggested that latitude might be a possible proxy to describe the variation of UV radiation over the TP. Additionally, from a global perspective, surface UV radiation increases with elevation due to the shorter distance of travel through the atmosphere (Sola et al., 2008), which may also have a negative influence on the atmospheric concentration of cVMS. Thus, elevation and latitude can be integrated together to simulate the effects of UV radiation (representing the influence of hydroxyl radicals) on concentrations of cVMS. On the other hand, latitude is also a factor that can represent the influence of emission sources; low-latitude regions will receive more cVMS due to their proximity to source regions (see Figure 2). Thus, an empirical model was derived here to estimate the combined effects of UV radiation and the distance to emission source regions on concentrations of cVMS:

$$C_{cVMS} = a + b\ Elevation + c\ Latitude \quad (2)$$

where a, b and c are coefficients determined from statistical regression. For the multiple linear regressions, the R^2 values can be used to explain the variation of the dependents. According to the correlations (the data from Lhasa and Golmud were excluded), the relationship can be described as in the following:

$$C_{cVMS} = 134 - 0.011\ Elevation - 2.35\ Latitude \quad (R^2 = 0.60, p < 0.01)$$

This means elevation and latitude can jointly explain 60% of the atmospheric concentration of cVMS. Other factors, such as cloud coverage and sky clarity (which influence hydroxyl radical levels in the air), may be the confounding factors that influence the correlation (Sola et al., 2008). The slope for elevation (*b*) is negative, suggesting that high concentrations of cVMS will occur at sites with low elevation, where hydroxyl radiation is limited. Two competing factors influence the coefficient for latitude. The contribution from the proximity to source regions means that the low-latitude regions of the TP will have high concentrations of cVMS (negative correlations between latitude and C_{cVMS}), due to these sites being close to the source regions of south Asia, while the strong hydroxyl degradation caused by UV radiation at low latitudes would have the opposite effect of reducing the concentrations of cVMS (positive correlation between latitude and C_{cVMS}). From the above model, the slope for latitude (*c*) in the model is also negative (−2.35), implying that the contribution from the proximity to source regions to concentrations of cVMS is broadly greater than that of hydroxyl degradation.

Correlations between cVMS congeners

Similar to previously published studies, good correlations were found between D3, D4, and D5 (Table S9). The correlation coefficients varied from 0.69 to 0.79 (all correlations were significant at the 95% confidence level; the data from Lhasa and Golmud were excluded), while the correlation between D5 and D6 was not significant. The good correlation implies that either D3, D4, and D5 have common sources and transport mechanisms, or there is chemical transformation to D3 and D4 from D5 (Kierkegaard et al., 2010).

Comparison of Measured and Modeled D5 Concentrations.

The measured D5 concentrations are compared with the concentrations predicted by the Danish Eulerian Hemispheric Model (DEHM, McLachlan et al., 2010). The country-based emissions were distributed into the DEHM grid according to a data set of the

gridded population density of the world with the total emission of D5 within the DEHM model domain estimated as 30 kT per year (McLachlan et al., 2010). All physical-chemical properties of D5 used in model prediction are reported in previous study (Brooke et al., 2009; Jiménez et al., 2005). The rate constant for the reaction of D5 with OH radicals measured by Atkinson (1991) was employed. NCEP (National Centers for Environmental Prediction) global analysis meteorological data are used to driven model. By comparing different scenarios, the DEHM model found that phototransformation is the dominant elimination process between emission of the D5 and arrival at the sampling site. There is good agreement between the spatial variability in D5 concentration between the measurements of the TP and the model prediction, displaying great D5 concentrations in southeast TP. The good tracking of the measured concentration by the DEHM shows that D5 is clearly subject to LRAT, although it is also effectively removed from the atmosphere via phototransformation. However, measured D5 concentrations are 1-3 magnitudes higher than the model prediction. Given atmospheric emission data of D5 in DEHM are estimated from usage of antiperspirant and skin creams, the emission uncertainties might lead to the discrepancy between measured concentrations and model values.

Implications

To the best of our knowledge, this is the first study on atmospheric concentrations of neutral PFASs and cVMS in the TP region. Due to the remoteness of the TP, the contamination of these emerging compounds will provide insight into how and to what extent the emissions in the source regions influence these last pieces of pristine land. Levels of neutral PFASs in the air of the TP are in the hundreds of pg/m^3, and levels of cVMS are in the ng/m^3 range. These values are 2–3 times and 1–2 orders of magnitude, respectively, higher than those for legacy chemicals (such as DDT and HCHs, with maximum concentrations in the tens of pg/m^3, Wang et al., 2016b). Moreover, among the various legacy and emerging POPs in wild Tibetan fishes, the average level of ΣPFASs is the third highest (just after those of ΣDDT and ΣHCHs, Shi et al., 2015; Wang et al., 2016a). All this evidence suggests that emerging POPs should be of great

concern for the environmental safety of the TP, as they are large volume production chemicals that have not been regulated in the surrounding countries. Due to the LRAT potential of volatile PFASs and cVMS, joint regulation of these emerging chemicals by south Asian counties (upwind of the TP) has been requested in order to protect the Tibetan environment. Taking data from this study and the pilot study for Asian countries (Li et al., 2011) into account, due to the growing population and the transfer of production factories from developed countries to Asian counties, Asian cities will increasingly be the sources of emerging POPs from a global perspective.

China has not strongly regulated the manufacture of PFASs or the use of personal care products. Over the last ten years, extensive urbanization has occurred in China. For example, the population in Lhasa reached 90,000 in 2015, having increased by 33% from 2014. It is estimated that the population in Lhasa will reach 110,000 in 2020. Thus, emissions of emerging compounds due to urbanization will inevitably increase. Following the population expansion, wastewater treatment plants deployed in cities will not only emit volatile PFASs and cVMS into the air, but will also contaminate the TP's water bodies (i.e. rivers, wetlands, and lakes), which are precious clean water resources. Thus, the risks posed by city expansion to the burden and transport of pollutants should be of great concern. Increasingly, concern regarding the toxicity and exposure risks of PFASs and cVMS is growing among scientists and regulators. This work has important implications for policymakers in comprehensively protecting the Tibetan alpine environment and promoting sustainable development in Tibet (the water tower of Asia).

Acknowledgements. This study was supported by the National Natural Science Foundation of China (41671480 and 41222010), Youth Innovation Promotion Association (CAS2011067) and the International Partnership Program of the Chinese Academy of Sciences (Grant No. 131C11KYSB20160061).

Reference

Ahrens, L., Harner, T., and Shoeib, M.: Temporal Variations of Cyclic and Linear Volatile Methylsiloxanes in the Atmosphere Using Passive Samplers and High-Volume Air Samplers, Environ. Sci. Technol., 48, (16), 9374-9381, 2014.

Ahrens, L., Harner, T., Shoeib, M., Koblizkova, M., and Reiner, E. J.: Characterization of Two Passive Air Samplers for Per- and Polyfluoroalkyl Substances: Environ. Sci. Technol., 47, 14024-14033, 2013.

Ahrens, L., Shoeib, M., Harner, T., Lane, D. A., Guo, R., and Reiner, E. J.: Comparison of Annular Diffusion Denuder and High Volume Air Samplers for Measuring Per- and Polyfluoroalkyl Substances in the Atmosphere, Anal. Chem., 84, 1797-1797, 2012.

Ahrens, L., Shoeib, M., Vento, S. D., Codling, G., and Halsall, C.: Polyfluoroalkyl compounds in the Canadian Arctic atmosphere: Environ. Chem., 8, 399-406, 2011.

Atkinson, R.: Kinetics of the gas-phase reactions of a series of organosilicon compounds with OH and NO sub 3 radicals and O sub 3 at 297 + 2K, Environ. Sci. Technol., 25, 863–866, 1991

Borga, K., Fjeld, E., Kierkegaard, A., and McLachlan, M. S.: Consistency in Trophic Magnification Factors of Cyclic Methyl Siloxanes in Pelagic Freshwater Food Webs Leading to Brown Trout: Environ. Sci. Technol., 47, 14394-14402, 2013.

Brooke, D. N., Crookes, M. J., Gray, D., and Robertson, S.: Environmental risk assessment report: Decamethylcyclopentasiloxane, Environment Agency of England and Wales, Bristol, 2009,.

Buser, A. M., Kierkegaard, A., Bogdal, C., MacLeod, M., Scheringer, M., and Hungerbühler, K.: Concentrations in Ambient Air and Emissions of Cyclic Volatile Methylsiloxanes in Zurich, Switzerland: Environ. Sci. Technol. 47, 7045-7051, 2013.

Butt, C. M., Berger, U., Bossi, R., and Tomy, G. T.: Levels and trends of poly- and perfluorinated compounds in the arctic environment: Sci. Total Environ., 408, 2936-2965, 2010.

Cai, M., Xie, Z., Möller, A., Yin, Z., Huang, P., Cai, M., Yang, H., Sturm, R., He, J., and Ebinghaus, R.: Polyfluorinated compounds in the atmosphere along a cruise pathway from the Japan Sea to the Arctic Ocean: Chemosphere, 87, 989-997, 2012.

European Chemical Agency (ECHA). Identification of PBT and vPvB substance. Results of evaluation of PBT/vPvB properties for decamethylcyclopentasiloxane; 2012 [Available online at http://echa.europa.eu/documents/10162/13628/decamethyl_pbtsheet_en.pdf].

Genualdi, S., Harner, T., Cheng, Y., MacLeod, M., Hansen, K. M., van Egmond, R., Shoeib, M., and Lee, S. C.: Global Distribution of Linear and Cyclic Volatile Methyl Siloxanes in Air: Environ. Sci. Technol., 45, 3349-3354, 2011.

Genualdi, S., Lee, S. C., Shoeib, M., Gawor, A., Ahrens, L., and Harner, T.: Global pilot study of legacy and emerging persistent organic pollutants using sorbent-impregnated polyurethane foam disk passive air samplers: Environ. Sci. Technol., 44, 5534-5539, 2010.

Guerranti, C., Perra, G., Corsolini, S., and Focardi, S. E.: Pilot study on levels of perfluorooctane sulfonic acid (PFOS) and perfluorooctanoic acid (PFOA) in selected foodstuffs and human milk from Italy: Food Chem. 140, 197-203, 2013.

Hogue, C.: Perfluorinated Chemical Controls: Chem. Engin. News, 90, 24-25, 2012.
Hung, H., Katsoyiannis, A. A., Brorström-Lundén, E., Olafsdottir, K., Aas, W., Breivik, K., Bohlin-Nizzetto, P., Sigurdsson, A., Hakola, H., Bossi, R., Skov, H., Sverko, E., Barresi, E., Fellin, P., and Wilson, S.: Temporal trends of Persistent Organic Pollutants (POPs) in arctic air: 20 years of monitoring under the Arctic Monitoring and Assessment Programme (AMAP): Environ. Pollut., 217, 52-61, 2016a.
Hung, H., Katsoyiannis, A. A., and Guardans, R.: Ten years of global monitoring under the Stockholm Convention on Persistent Organic Pollutants (POPs): Trends, sources and transport modelling: Environ. Pollut., 217, 1-3, 2016b.
Jiménez, E., Ballesteros, B., Martínez, E., and Albaladejo, J.: Tropospheric reaction of OH with selected linear ketones: kinetic studies between 228 and 405 K: Environ. Sci. Technol., 39, 814-820, 2005.
Kierkegaard, A., Adolfsson-Erici, M., and McLachlan, M. S.: Determination of Cyclic Volatile Methylsiloxanes in Biota with a Purge and Trap Method: Anal. Chem., 82, 9573-9578, 2010.
Krogseth, I. S., Kierkegaard, A., McLachlan, M. S., Breivik, K., Hansen, K. M., and Schlabach, M.: Occurrence and Seasonality of Cyclic Volatile Methyl Siloxanes in Arctic Air, Environ. Sci. Technol.47, 502-509, 2013.
Li, J., Vento, S. D., Schuster, J., Zhang, G., Chakraborty, P., Kobara, Y., and Jones, K. C.: Perfluorinated Compounds in the Asian Atmosphere, Environ. Sci. Technol., 45, 7241-7246, 2011.
Liu, H., Bo, H. U., Wang, Y., Liu, G., Tang, L., Dongsheng, J. I., Bai, Y., Bao, W., Chen, X., and Chen, Y.: Two Ultraviolet Radiation Datasets that Cover China, Adv. Atmos. Sci., 34, 805-815, 2017.
Mackay, D.: Risk assessment and regulation of D5 in Canada: Lessons learned: Environ. Toxicol. Chem., 34, 2687-2688, 2015.
Mackay, D., Powell, D. E., and Woodburn, K. B.: Bioconcentration and Aquatic Toxicity of Superhydrophobic Chemicals: A Modeling Case Study of Cyclic Volatile Methyl Siloxanes: Environ. Sci. Technol., 49, 11913-11922, 2015.
Magulova, K., and Priceputu, A.: Global monitoring plan for persistent organic pollutants (POPs) under the Stockholm Convention: Triggering, streamlining and catalyzing global POPs monitoring: Environ. Pollut., 217, 82-84, 2016.
McGoldrick, D. J., Chan, C., Drouillard, K. G., Keir, M. J., Clark, M. G., and Backus, S. M.: Concentrations and trophic magnification of cyclic siloxanes in aquatic biota from the Western Basin of Lake Erie, Canada: Environ. Pollut., 186, 141-148, 2014.
McLachlan, M. S., Kierkegaard, A., Hansen, K. M., van Egmond, R., Christensen, J. H., and Skjøth, C. A.: Concentrations and Fate of Decamethylcyclopentasiloxane (D5) in the Atmosphere, Environ. Sci. Technol., 44, 5365-5370, 2010.
Navea, J. G., Young, M. A., Xu, S., Grassian, V. H., and Stanier, C. O.: The atmospheric lifetimes and concentrations of cyclic methylsiloxanes octamethylcyclotetrasiloxane (D4) and decamethylcyclopentasiloxane (D5) and

610 the influence of heterogeneous uptake: Atmos. Environ., 45, 3181-3191, 2011.
611 Nguyen, M. A., Wiberg, K., Ribeli, E., Josefsson, S., Futter, M., Gustavsson, J., and
612 Ahrens, L.: Spatial distribution and source tracing of per- and polyfluoroalkyl
613 substances (PFASs) in surface water in Northern Europe: Environ. Pollut., 220.
614 1438-1446, 2016.
615 Paul, A. G., Jones, K. C., and Sweetman, A. J.: A first global production, emission, and
616 environmental inventory for perfluorooctane sulfonate, Environ. Sci. Technol.,
617 43, 386-392, 2009.
618 Pedersen, K. E., Letcher, R. J., Sonne, C., Dietz, R., and Styrishave, B.: Per- and
619 polyfluoroalkyl substances (PFASs) – New endocrine disruptors in polar bears
620 (Ursus maritimus)? Environ. Intern., 96, 180-189, 2016.
621 Piekarz, A. M., Primbs, T., Field, J. A., Barofsky, D. F., and Simonich, S.: Semivolatile
622 Fluorinated Organic Compounds in Asian and Western U.S. Air Masses:
623 Environ. Sci. Technol., 41, 8248-8255, 2007.
624 Pozo, K., Harner, T., Lee, S. C., Wania, F., Muir, D. C. G., and Jones, K. C.: Seasonally
625 Resolved Concentrations of Persistent Organic Pollutants in the Global
626 Atmosphere from the First Year of the GAPS Study, Environ. Sci. Technol., 43,
627 796-803, 2009.
628 Qiu, J.: China: The third pole: Nature,. 454, 393, 2008
629 Rayne, S., Forest, K., and Friesen, K. J.: Estimated congener specific gas-phase
630 atmospheric behavior and fractionation of perfluoroalkyl compounds: rates of
631 reaction with atmospheric oxidants, air-water partitioning, and wet/dry
632 deposition lifetimes: J. Environ. Sci. Health Part A 44, 936-954, 2009.
633 Ren, J., Wang, X., Wang, C., Gong, P., Wang, X., and Yao, T.: Biomagnification of
634 persistent organic pollutants along a high-altitude aquatic food chain in the
635 Tibetan Plateau: Processes and mechanisms: Environ. Pollut., 220, 636-642,
636 2016,
637 Rigét, F., Bignert, A., Braune, B., Stow, J., and Wilson, S.: Temporal trends of legacy
638 POPs in Arctic biota, an update: Sci. Total Environ., 408, 2874-2884, 2010.
639 Rohrer, F., and Berresheim, H.: Strong correlation between levels of tropospheric
640 hydroxyl radicals and solar ultraviolet radiation: Nature, 442, 184, 2006.
641 Sanchís, J., Cabrerizo, A., Galbán-Malagón, C., Barceló, D., Farré, M., and Dachs, J.:
642 Unexpected Occurrence of Volatile Dimethylsiloxanes in Antarctic Soils,
643 Vegetation, Phytoplankton, and Krill: Environ. Sci. Technol., 49, 4415-4424,
644 2015.
645 Sharma, B. M., Bharat, G. K., Tayal, S., Larssen, T., Bečanová, J., Karásková, P.,
646 Whitehead, P. G., Futter, M. N., Butterfield, D., and Nizzetto, L.: Perfluoroalkyl
647 substances (PFAS) in river and ground/drinking water of the Ganges River
648 basin: Emissions and implications for human exposure, Environ. Pollut., 208,
649 704-713, 2016.
650 Sheng, J., Wang, X., Gong, P., Joswiak, D. R., Tian, L., Yao, T., and Jones, K. C.:
651 Monsoon-driven transport of organochlorine pesticides and polychlorinated
652 biphenyls to the Tibetan Plateau: three year atmospheric monitoring study:
653 Environ. Sci. Technol., 47, 3199-3208, 2013.

Shi, Y., Xu, S., Xu, L., and Cai, Y.: Distribution, Elimination, and Rearrangement of Cyclic Volatile Methylsiloxanes in Oil-Contaminated Soil of the Shengli Oilfield, China, Environ. Sci. Technol., 49, 11527-11535, 2015.

Shoeib, M., Harner, T., Lee, S. C., Lane, D., and Zhu, J. P.: Sorbent-impregnated polyurethane foam disk for passive air sampling of volatile fluorinated chemicals: Anal. Chem., 80, 675-682, 2008.

Shoeib, M., Harner, T., and Vlahos, P.: Perfluorinated chemicals in the arctic atmosphere: Environ. Sci. Technol.,40, 7577-7583, 2006.

Sola, Y., Lorente, J., Campmany, E., De Cabo, X., Bech, J., Redaño, A., Martínez‐Lozano, J. A., Utrillas, M. P., Alados‐Arboledas, L., and Olmo, F. J.: Altitude effect in UV radiation during the Evaluation of the Effects of Elevation and Aerosols on the Ultraviolet Radiation 2002 (VELETA‐2002) field campaign: J. Geophy. Res. Atmos. 113, 1323-1330, 2008.

Wang, D.-G., Aggarwal, M., Tait, T., Brimble, S., Pacepavicius, G., Kinsman, L., Theocharides, M., Smyth, S. A., and Alaee, M.: Fate of anthropogenic cyclic volatile methylsiloxanes in a wastewater treatment plant: Water Res. 72, 209-217, 2015a,

Wang, X., Gong, P., Wang, C., Ren, J., and Yao, T.: A review of current knowledge and future prospects regarding persistent organic pollutants over the Tibetan Plateau: Sci. Total Environ., 573, 139-154, 2016a.

Wang, X., Gong, P., Yao, T., and Jones, K. C.: Passive air sampling of organochlorine pesticides, polychlorinated biphenyls, and polybrominated diphenyl ethers across the Tibetan plateau: Environ. Sci. Technol., 44, 2988-2993, 2010.

Wang , X., Halsall, C., Codling, G., Xie, Z. g., Xu, B., Zhao, Z., Xue, Y., Ebinghaus, R., and Jones, K. C.: Accumulation of perfluoroalkyl compounds in tibetan mountain snow: temporal patterns from 1980 to 2010: Environ. Sci. Technol., 48, 173-181, 2014.

Wang, X., Ren, J., Gong, P., Wang, C., Xue, Y., Yao, T., and Lohmann, R.: Spatial Distribution of the Persistent Organic Pollutants across the Tibetan Plateau and Its Linkage with the Climate Systems: Five Year Air Monitoring Study: Atmos. Chem. Phys. 16, 6901-6911, 2016b.

Wang, Z., Xie, Z., Mi, W., Möller, A., Wolschke, H., and Ebinghaus, R.: Neutral poly/per-fluoroalkyl substances in air from the Atlantic to the Southern Ocean and in Antarctic snow, Environ. Sci. Technol., 49, 7770-7775, 2015b.

Xiao, R., Zammit, I., Wei, Z., Hu, W.-P., MacLeod, M., and Spinney, R.: Kinetics and Mechanism of the Oxidation of Cyclic Methylsiloxanes by Hydroxyl Radical in the Gas Phase: An Experimental and Theoretical Study, Environ. Sci. Technol., 49, 13322-13330, 2015.

Xu, S., Kozerski, G., and Mackay, D.: Critical Review and Interpretation of Environmental Data for Volatile Methylsiloxanes: Partition Properties: Environ. Sci. Technol., 48, 11748-11759, 2014.

Xu, S., and Wania, F.: Chemical fate, latitudinal distribution and long-range transport of cyclic volatile methylsiloxanes in the global environment: A modeling assessment: Chemosphere, 93, 835-843, 2013.

698 Zushi, Y., Hogarh, J. N., and Masunaga, S.: Progress and perspective of perfluorinated
699 compound risk assessment and management in various countries and institutes:
700 Clean Technol. Environ. Policy, 14, 9-20, 2012.

701

Table 1 Description of the sampling program

Sampling site	Longitude	Latitude	Elevation /m; Temperature/°C	Description	Date of sample collection	
					2011	2013
Bomi	E 95°46.167′	N 29°51.485′	2720; 8.8	Hydrological observation station, remote area	05/02–07/28	05/05–07/25
Rawu	E 96°54.745′	N 29°22.289′	4540; -2	Rural site, 20 km from Rawu Lake	05/03–07/31	05/05–07/26
Lunang	E 94°44.246′	N 29°45.908′	3330; 5.4	Meteorological station in forest region, remote area	05/02–07/28	05/05–07/31
Qamdo	E 97°08.624′	N 31°09.014′	3250; 7.6	Rural site, 50 km from farm land	05/04–07/31	05/06–07/28
Chayu	E97°29.4′	N 28°37.2′	1400; 12.4	Meteorological station, remote area	05/05–07/31	05/02–07/29
Nam Co	E 90°57.800′	N 30°46.375′	4740; -2.2	Meteorological station near the Nam Co lake, remote area	05/05–07/25	05/05–07/31
GBJD	E 93°14.478′	N 29°53.122′	3420; 6.2	Hydrological observation station, remote area	05/03–07/28	05/04–07/28
Lhasa	E 91°01.956′	N 29°38.728′	3660; 8.1	Building roof of the Lhasa campus	05/01–07/31	05/08–07/28
Lhaze	E 87°38.094′	N 29°05.405′	4020; 6.8	Meteorological station, rural site	05/02–07/31	05/04–07/27
Xigaze	E 88°53.319′	N 29°15.014′	3840; 6.6	Meteorological station, rural site	05/03–07/31	05/05–07/24
Mt. Everest	E 86°56.948′	N 28°21.633′	4300; 4.3	Meteorological station near the Mt. Everest, remote area	05/02–07/31	05/03–07/29
Saga	E 85°13.951′	N 29°19.889′	4500; 6.5	Rural site and without agriculture activities	05/07–07/25	05/06–07/28
Golmud	E 94°54.480′	N 36°23.637′	2830; 5.3	Observation station for frost soil, rural site	05/02–07/27	05/06–07/27
Naqu	E 91°58.827′	N 31°25.373′	4500; -1	Hydrological observation station, remote area	05/02–07/31	05/05–07/26
Gar	E 80°05.654′	N 32°30.116′	4300; 0.6	Meteorological station, remote area	05/06–07/31	05/03–07/27
Muztagata	E 74°50.919′	N 38°16.072′	5200; -6	Meteorological station, remote area	05/09–07/31	05/07–07/29

702

703

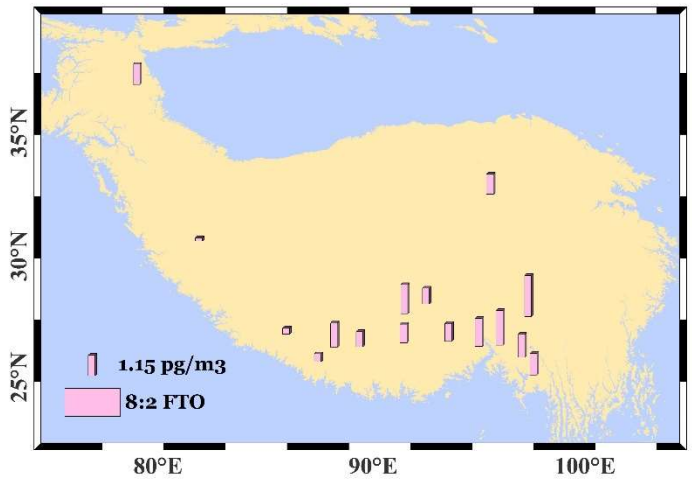

704

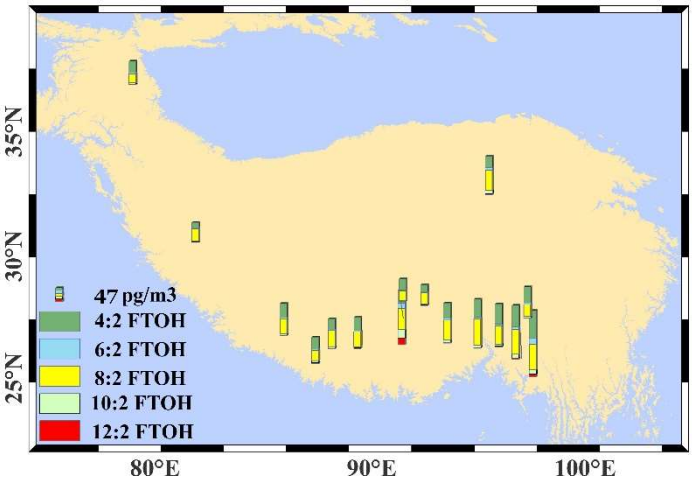

705

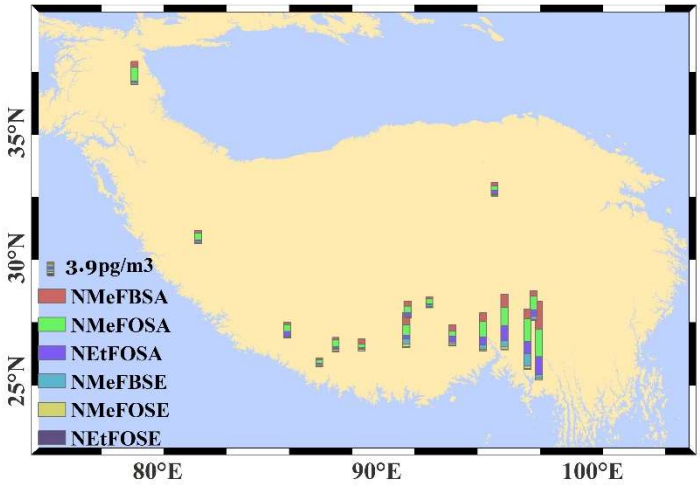

706 **Figure 1 Spatial distribution of neutral PFASs in the atmosphere of the TP**

Table 2 Correlation (*r*) of individual compounds among all the samples

	4:2 FTOH	6:2 FTOH	8:2 FTOH	10:2 FTOH	12:2 FTOH	NMeFBSA	NMeFOSA	NEtFOSA	NMeFBSE	NMeFOSE	NEtFOSE
8:2 FTO	0.44	0.12	0.18	0.04	0.00	0.32	0.46	0.44	0.37	0.20	−0.11
4:2 FTOH		**0.62**	0.49	0.37	0.25	**0.84**	**0.84**	**0.92**	*0.56*	0.42	−0.17
6:2 FTOH			**0.68**	*0.59*	**0.84**	**0.84**	*0.60*	*0.57*	0.39	*0.62*	−0.32
8:2 FTOH				**0.90**	0.45	**0.63**	*0.57*	*0.67*	*0.58*	**0.63**	−0.33
10:2 FTOH					**0.97**	*0.58*	0.35	0.30	0.42	**0.77**	−0.21
12:2 FTOH						*0.52*	0.26	0.19	0.33	**0.71**	−0.14
NMeFBSA							**0.83**	**0.84**	0.44	0.42	−0.24
NMeFOSA								**0.88**	**0.69**	0.43	−0.24
NEtFOSA									**0.63**	0.37	−0.03
NMeFBSE										**0.75**	−0.03
NMeFOSE											−0.13

Bold and italic are significant at $p < 0.01$ and $p < 0.05$, respectively.

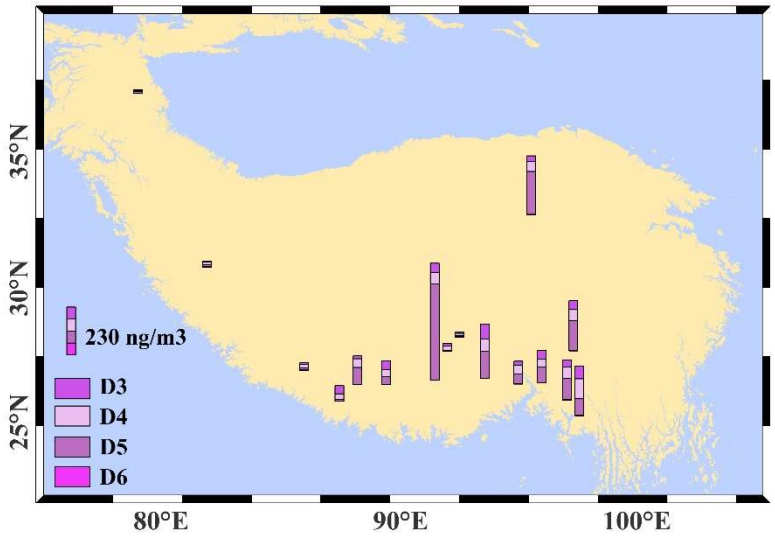

Figure 2 Spatial distribution of cVMS in the atmosphere of the TP